Pulse width-modulated switching strategy for the dynamic balancing of zero-sequence current for a dual-inverter fed open-end winding induction motor drive

V.T. Somasekhar, S. Srinivas, B. Prakash Reddy, Ch. Nagarjuna Reddy and K. Sivakumar

Abstract: Three-level inversion can be achieved with dual two-level inverters feeding an open-end winding induction motor. A space vector-based pulse width-modulated (PWM) switching scheme is proposed, which achieves three-level inversion using all the space vector locations with a single DC power supply. The zero-sequence current is reduced by reducing the zero-sequence voltage to zero, in the average sense, within a sampling time interval. The proposed PWM scheme balances the zero-sequence current dynamically, simply with a relocation of the effective time within a sampling time interval. The switching frequency of the inverters is also reduced to half as only one inverter is switched while the other is clamped in a sampling time interval. Also, the proposed PWM scheme employs only the three instantaneous phase reference voltages obviating the necessity of sector identification and lookup tables.

1 Introduction

Multi-level pulse width-modulated (PWM) inverters gained increased interest in the recent past and various multi-level inverter topologies have been suggested [1–6]. Three-level inversion, realised with dual two-level inverters feeding an open-end winding induction motor, has aroused the interest of various researchers in the last few years. This configuration offers advantages such as more redundant space vector combinations, absence of fluctuating DC neutral point and the avoidance of clamping diodes when compared with the conventional three-level NPC inverter. However, two isolated DC power supplies are required to feed individual inverters in this power circuit topology to employ all the space vector locations.

A sine-triangle modulation technique for the control of inverters was used for the open-end winding induction motor [6]. A space vector modulation technique was suggested [7], in which two isolated DC power supplies were used to supply the two inverters feeding the open-end winding induction motor which would deny the path for the zero-sequence current. The zero-sequence voltage which causes the zero-sequence current can be reduced or eliminated altogether. To this effect, a number of PWM schemes are suggested [8–15]. In the work reported in Somasekhar *et al*. [10], Baiju *et al*. [11] and Oleschuk *et al*. [12], the zero-sequence voltage is altogether avoided by employing only those space vector combinations for which the zero-sequence voltage is zero. However, the resulting inverter is not a three-level inverter in the strictest sense as all the space vector locations are not used resulting in the underutilisation of the switching resources.

Recently, a new circuit topology was suggested for the dual two-level inverter fed open-end winding induction motor with auxiliary switches for three-level inversion and used a single DC power supply [8, 9]. The auxiliary switches create an isolated switching neutral denying a path for the zero-sequence current. This again would require additional switches that increase the cost of the drive and also increase the complexity of control.

In this paper, it is shown that three-level inversion is possible, in principle, with only one DC power supply for an open-end winding induction motor drive without employing the additional auxiliary switches. The PWM strategy suggested in this work uses all the space vector locations. The effective time concept proposed in Kim and Sul [16] and Chung *et al*. [17] is extended to a dual-inverter driven open-end winding induction motor drive. In the proposed PWM scheme, the actual gating times for the inverter devices are obtained by a simple relocation of the effective time period in the sampling time interval. The proposed PWM scheme eliminates additional hardware requirements such as auxiliary switches. Specifically, the PWM scheme proposed in this paper significantly reduces the zero-sequence current by dynamically balancing the zero-sequence voltages, by the effective time relocation algorithm.

2 Dual-inverter with the single DC power supply

The schematic of a dual two-level inverter fed three-phase open-end winding induction motor fed from a single power supply is shown in Fig. 1.

In this scheme, each of the dual two-level inverters can produce eight space vector locations independent of the other as shown in Fig. 2*a*, resulting in a total of 64 space vector combinations spread over the 19 space locations as shown in Fig. 2*b* [8]. The numbers 1–8 denote the states

doi:10.1049/iet-epa:20060407

Paper first received 16th October and in revised form 4th December 2006

The authors are with the Department of Electrical Engineering, National Institute of Technology, Warangal 506 004, India

E-mail: vtsomasekhar@rediffmail.com

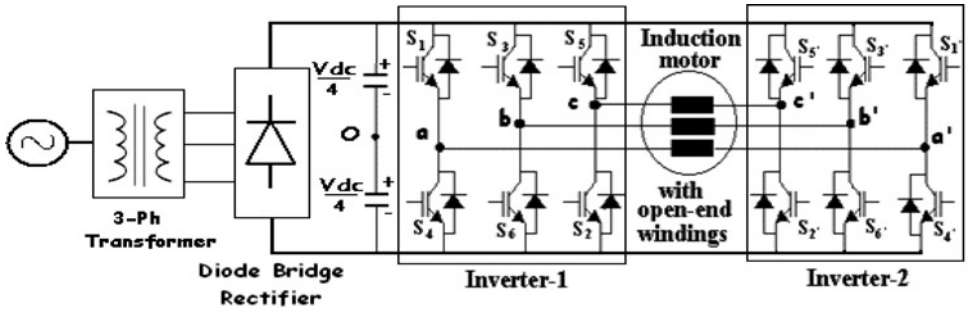

Fig. 1 *Dual two-level inverter with a single DC power supply*

assumed by inverter-1 and $1'-8'$ denotes the same for inverter-2. The switching states of the two inverters are tabulated in Table 1.

A '+' indicates that the top switching device in a leg of a given inverter is turned 'ON', whereas a '−' indicates that the bottom switching device in a leg of the given inverter is turned 'ON'. The symbols v_{ao}, v_{bo} and v_{co} denote the three phase pole voltages of inverter-1 whereas the symbols $v_{a'o}$, $v_{b'o}$ and $v_{c'o}$ denote the same for inverter-2 as in Fig. 1. In the same figure, |OA| represents the DC link voltage of individual inverters which is equal to $V_{dc}/2$ and |OG| represents the DC link voltage of the equivalent three-level inverter which is equal to V_{dc}. From Fig. 2*b* it may be seen that there are 19 space vector locations, which form vertices of 24 equilateral sectors. Six hexagons namely OBHGSF, OCJIHA, ODLKJB, OENMLC, OFQPND and OASRQE may be identified with their centers at A, B, C, D, E and F respectively, within the outer hexagon GIKMPR. For the rest of this paper, these points are called as sub-hexagonal centers (SHCs). The SHC, which is situated in the closest proximity to the tip of the reference voltage space vector, is termed as the nearest sub-hexagonal center (NSHC). As the two inverters are fed from the common DC link, without two separate DC power supplies, the zero-sequence current is expected to flow. The zero-sequence voltage which causes the zero-sequence current in the motor phases is defined as

$$v_{ZS} \equiv \frac{1}{3}(v_{aa'} + v_{bb'} + v_{cc'})$$

For example, the switching combination required to realise the space vector located at G, is $14'$, the zero-sequence

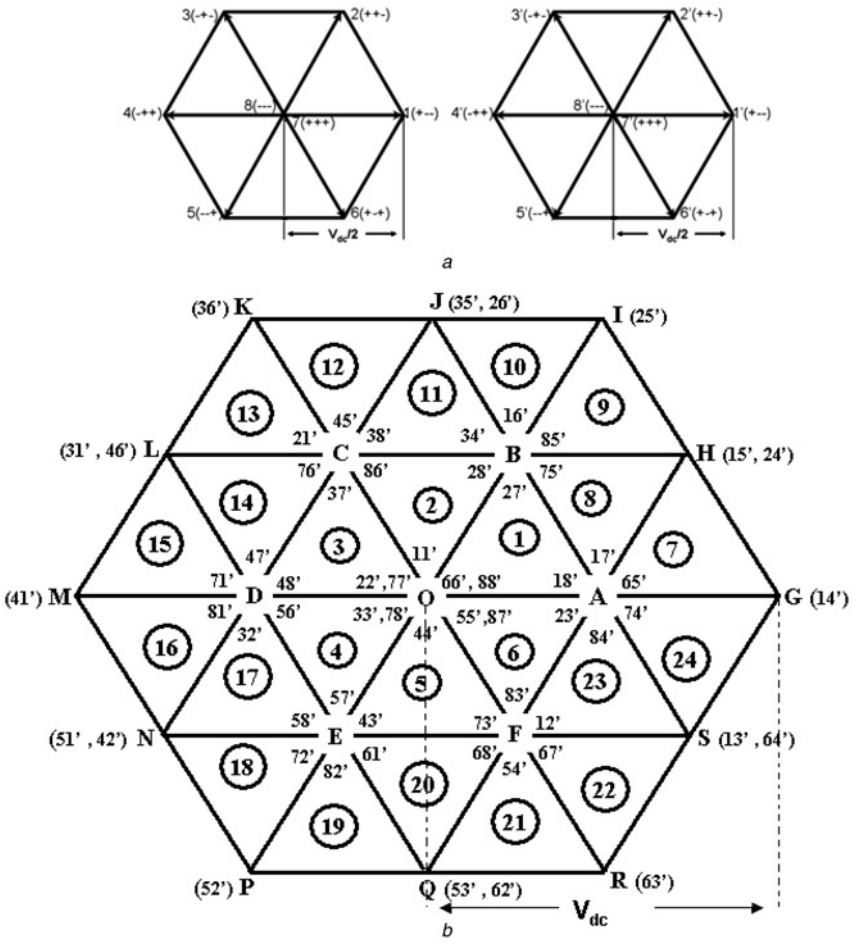

Fig. 2 *Space vector locations [VPN]*

a Space vector locations of the dual two-level inverters (top)
b Space vector locations with the combinations of the dual-inverter scheme (bottom)

Table 1: Switching states of the two inverters

State of inverter-1	Switches turned on	State of inverter-2	Switches turned on
1 (+ − −)	S_6, S_1, S_2	1′ (+ − −)	$S_{6'}$, $S_{1'}$, $S_{2'}$
2 (++−)	S_1, S_2, S_3	2′ (++−)	$S_{1'}$, $S_{2'}$, $S_{3'}$
3 (− + −)	S_2, S_3, S_4	3′ (− + −)	$S_{2'}$, $S_{3'}$, $S_{4'}$
4 (− ++)	S_3, S_4, S_5	4′ (− ++)	$S_{3'}$, $S_{4'}$, $S_{5'}$
5 (−−+)	S_4, S_5, S_6	5′ (−−+)	$S_{4'}$, $S_{5'}$, $S_{6'}$
6 (+ − +)	S_5, S_6, S_1	6′ (+ − +)	$S_{5'}$, $S_{6'}$, $S_{1'}$
7 (+++)	S_1, S_3, S_5	7′ (+++)	$S_{1'}$, $S_{3'}$, $S_{5'}$
8 (−−−)	S_2, S_4, S_6	8′ (−−−)	$S_{2'}$, $S_{4'}$, $S_{6'}$

voltage with this switching combination is calculated as follows

$$v_{aa'} = v_{ao} - v_{a'o} = \left(+\frac{V_{dc}}{4}\right) - \left(-\frac{V_{dc}}{4}\right) = \frac{V_{dc}}{2}$$

Similarly

$$v_{bb'} = v_{bo} - v_{b'o} = \left(-\frac{V_{dc}}{4}\right) - \left(+\frac{V_{dc}}{4}\right) = -\frac{V_{dc}}{2}$$

and

$$v_{cc'} = v_{co} - v_{c'o} = \left(-\frac{V_{dc}}{4}\right) - \left(+\frac{V_{dc}}{4}\right) = -\frac{V_{dc}}{2}$$

$$\therefore v_{ZS} \equiv \frac{1}{3}(v_{aa'} + v_{bb'} + v_{cc'})$$

$$= \frac{1}{3}\left(\frac{V_{dc}}{2} - \frac{V_{dc}}{2} - \frac{V_{dc}}{2}\right) = -\frac{V_{dc}}{6}$$

The zero-sequence content contributions from the 64 space vector switching combinations are shown in Table 2.

3 PWM switching scheme with dynamic balancing of zero-sequence voltage

The reference space vector for the space vector modulation is denoted as v_{sr} is resolved into two components v_α and v_β. The voltages v_a^*, v_b^* and v_c^* denote the instantaneous phase reference voltages required for realising v_{sr}. They are obtained by projecting the tip of v_{sr} onto a, b and c-phase-axes, respectively, and are given by the classical phase transformation as given below

$$\begin{bmatrix} v_a^* \\ v_b^* \\ v_c^* \end{bmatrix} = \begin{bmatrix} 2/3 & 0 \\ -1/3 & 1/\sqrt{3} \\ -1/3 & -1/\sqrt{3} \end{bmatrix} \begin{bmatrix} v_\alpha^* \\ v_\beta^* \end{bmatrix}$$

In this paper, a space vector-based PWM scheme is proposed which is based on the PWM scheme proposed in Kim and Sul [16]. From Kim and Sul [16], the symbols T_1 and T_2 denote the time duration for which the active vectors along the leading and trailing edges of the sector in which the tip of v_{sr} is situated are switched for its realisation. The symbol T_0 denotes the time duration for which the null vector is switched along with the active vectors. The sampling interval T_s for this space vector modulation is equal to the sum of the time durations, T_1, T_2 and T_0. The symbols T_{ga}, T_{gb} and T_{gc}, respectively, denote the a, b and c-phase switching time periods during which the output phases of the inverter are connected to the positive rail of the DC link.

The basic switching algorithm described in Kim and Sul [16] for the classical two-level inverter feeding three-phase induction motor is extended to the dual-inverter system for computing the switching times of the switching devices of the dual-inverter. This switching algorithm, is based on the imaginary switching time periods T_{as}, T_{bs} and T_{cs} which are proportional to the three instantaneous phase reference voltages v_a^*, v_b^* and v_c^*, the constant of proportionality being equal to (T_s/V_{dc}) [16]. The symbols T_{max}, T_{mid} and T_{min}, respectively, denote the maximum, median and minimum values among the three imaginary switching times. Recently, a space vector-based PWM switching scheme for the three-level, dual-inverter fed open-end winding induction motor was proposed using this switching algorithm [14]. The power circuit in Somasekhar *et al.* [14] consists of two isolated DC power supplies feeding the two inverters to deny the path for the zero-sequence current. This switching is briefly reviewed in the following paragraph.

The principle of the alternate PWM switching scheme is shown in Fig. 3. From Fig. 3, it can be seen that the reference vector OV can be split into two components namely OA and AV. The component OA is obtained by inverter-1 and the other component AV is realised in the average sense by switching inverter-2 around the SHC 'A'. In this switching scheme, if the NSHC is either 'A' or 'C' or 'E' then inverter-1 is chosen as clamping inverter and inverter-2, as switching inverter. At the other NSHCs ('B' or 'D' or 'F'), inverter-2 is chosen as the clamping inverter and inverter-1 as the switching inverter. Thus, the clamping and the switching inverters alternate their roles with the change in the NSHC. The selection of the clamping inverter and its clamping state entirely depend on NSHC. The NSHC is found based only on the three instantaneous reference voltage magnitudes [15]. Table 3 summarises the role of the two inverters under all the six SHCs [14]. The shaded region in Fig. 3 shows the area under the vicinity of the SHC 'A'. Should the sample lie in this region, inverter-1 is clamped and inverter-2 will be switched.

Table 2: Zero-sequence voltage contributions from different combinations

$-V_{dc}/2$	$-V_{dc}/3$	$-V_{dc}/6$	0	$+V_{dc}/6$	$+V_{dc}/3$	$+V_{dc}/2$
		8–5′, 8–3′		5–8′, 3–8′		
	8–4′	5–4′, 3–4′	8–8′, 5–5′, 5–3′, 3–5′,	4–5′, 4–3′	4–8′	
	8–6′	8–1′, 5–6′	3–3′, 4–4′, 5–1′, 3–1′,	4–1′, 1–8′	6–8′	
	8–2′	5–2′, 3–6′	4–6′, 4–2′, 1–5′, 1–3′	6–5′, 6–3′	2–8′	
8–7′	5–7′	3–2′, 4–7′	6–4′, 2–4′, 1–1′, 6–6′	2–5′, 2–3′	7–5′	7–8′
	3–7′	1–4′, 1–6′	6–2′, 2–6′, 2–2′, 7–7′	7–4′, 6–1′	7–3′	
	1–7′	1–2′, 6–7′		2–1′, 7–6′	7–1′	
		2–7′		7–2′		

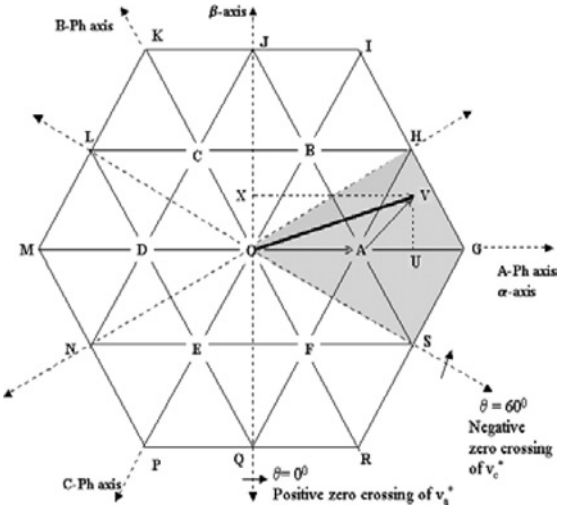

Fig. 3 *Principle of alternate-sub-hexagonal centre*

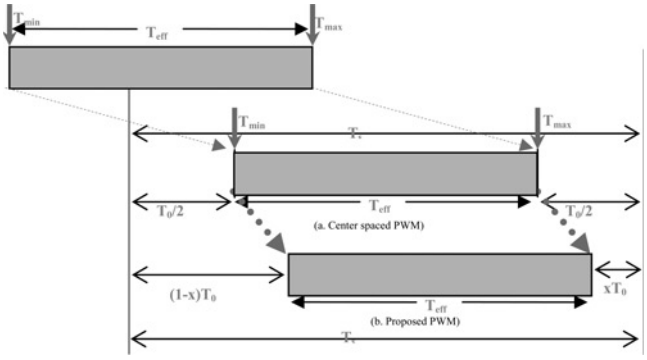

Fig. 4 *Effective time placement*

a Effective time placement in the centre of sampling interval
b Effective time relocation within the sampling time interval

Under the SHC 'A', inverter-1 is clamped and inverter-2 is switched. The tip of the reference vector can lie in any of the six sectors 1, 8, 7, 24, 23 or 6 (Fig. 2*b*). Should the tip of the reference vector lie in the sectors 1, 8 or 7, the mapped sectors for the switching inverter (inverter-2 here) would be 3, 2 or 1 respectively. For the dual-inverter, the switching combinations then available would be (17′–16′–11′–18′), (17′–16′–15′–18′) or (17′–14′–15′–18′) all for the OFF sequence which depend on the location of the tip of the reference vector in the sectors 1, 8 or 7. For example, if the tip of the reference vector is situated in sector 8, then the selected combination is (17′–16′–15′–18′). Therefore, inverter-1 is clamped to state 1(+ − −) and inverter-2 is switched between the states (7–6–5–8) for $(T_0/2 - T_2 - T_1 - T_0/2)$ duration, respectively, for the center-spaced PWM switching technique. The zero vector or null vector period (T_0) is uniformly divided into two null vector periods ($T_0/2$) leaving the effective time, $T_{\text{eff}} = \max\{T_{as}, T_{bs} \& T_{cs}\} - \min\{T_{as}, T_{bs} \& T_{cs}\}$ [16] exactly in the center of the sampling interval T_s. The effective time is the time during which the active vectors are used. This is achieved by giving a suitable time-shift to the imaginary switching times in the PWM scheme proposed in Somasekhar *et al*. [14] and is shown in Fig. 4*a*. The switching combinations are obtained in a similar manner when the tip of the reference vector lies in the sectors 24, 23 or 6 under the NSHC 'A'. In contrast with the above scheme, in the PWM scheme proposed in this paper, the zero vector period is dynamically changed within the sampling interval without changing the effective time. Unlike the aforementioned PWM scheme, in this scheme the time period T_0 is redistributed into two unequal time periods, $(1 - x)T_0$ and xT_0 respectively, such that the zero-sequence voltage is forced to be zero in the average sense for one sampling time interval. This redistribution of the null-vector period is pictorially represented in Fig. 4*b*. This effective time is symmetrically placed in the sampling interval for ON sequence. The placement of the effective time in two sampling intervals both for ON & OFF sequence are shown in Fig. 5.

When the tip of the reference vector is situated in sector 8 then the switching combinations used are (17′–16′–15′–18′), the mapped sector here would be 2 (for inverter-2). From Table 2, it is clear that the zero-sequence voltage contributions for the above switching combinations are, respectively, $(-V_{\text{dc}}/3)$, $(-V_{\text{dc}}/6)$, (0) and $(+V_{\text{dc}}/6)$. In order to eliminate the zero-sequence voltages within the sampling interval in the average sense, the zero-sequence volt-seconds is forced equal to zero. That is

$$\left[\left(-\frac{V_{\text{dc}}}{3}\right) \times (1-x)T_0\right] + \left[\left(-\frac{V_{\text{dc}}}{6}\right) \times T_2\right] + [(0) \times T_1] + \left[\left(+\frac{V_{\text{dc}}}{6}\right) \times xT_0\right] = 0 \quad (1)$$

$$\Rightarrow -\frac{T_0}{3} + \frac{xT_0}{3} - \frac{T_2}{6} + \frac{xT_0}{6} = 0$$

$$\therefore xT_0 = \frac{2T_0}{3} + \frac{T_2}{3} \quad (2a)$$

$$\therefore x = \frac{2}{3} + \frac{T_2}{T_0} \quad (0 \le x \le 1) \quad (2b)$$

T_{offset} is the time-shift given to the imaginary switching times to obtain the actual gating signals to the top devices of the switching inverter [16]. It is shown in Kim and Sul [16] that the offset time required to place the effective time block at the centre of T_s is given by $(T_0/2 - T_{\min})$. The time shift that would be required for balancing the zero sequence volt-seconds is derived as (Figs. 4 and 5)

$$T_{\text{offset}} = (1-x)T_0 - T_{\min} = T_0 - xT_0 - T_{\min} \quad (3)$$

Table 3: Inverter roles for realizing the reference vector

NSHC	A	B	C	D	E	F
inverter-1	clamped to state 1 (+ − −)	switching mode	clamped to state 3 (− + −)	switching mode	clamped to state 5 (− − +)	switching mode
inverter-2	switching mode	clamped to state 5 (− − +)	switching mode	clamped to state 1 (+ − −)	switching mode	clamped to state 3 (− + −)

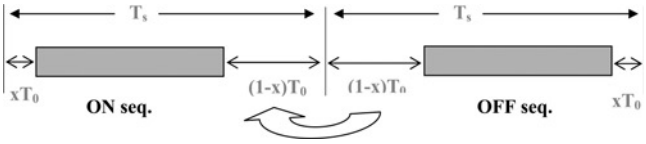

Fig. 5 *Effective time placement in two sampling intervals for both ON and OFF sequence*

Putting (2a) into (3), we have

$$T_{\text{offset}} = T_0 - \left(\frac{2T_0}{3} + \frac{T_2}{3}\right) - T_{\min}$$
$$= \frac{T_0}{3} - \frac{1}{3}(T_{\text{mid}} - T_{\min}) - T_{\min}$$
$$= T_0 - \frac{2T_0}{3} - \frac{T_2}{3} - T_{\min}$$
$$= \frac{T_0}{3} - \frac{T_{\text{mid}}}{3} + \frac{T_{\min}}{3} - T_{\min} \quad (4)$$

$$\because T_{\max} + T_{\text{mid}} + T_{\min} = 0$$
$$T_{\min} = -(T_{\max} + T_{\text{mid}}) \quad (5)$$

Putting equation (5) in equation (4), we have

$$T_{\text{offset}} = \frac{T_0}{3} - \frac{1}{3}(-T_{\max} - T_{\min}) + \frac{T_{\min}}{3} - T_{\min}$$
$$= \frac{T_0}{3} + \frac{1}{3}(T_{\max} + T_{\min}) - \frac{2T_{\min}}{3}$$
$$= \frac{T_0}{3} + \frac{T_{\max}}{3} + \frac{T_{\min}}{3} - \frac{2T_{\min}}{3}$$
$$= \frac{T_0}{3} + \frac{1}{3}(T_{\max} - T_{\min})$$
$$\because T_{\max} - T_{\min} = T_{\text{eff}}$$
$$T_{\text{offset}} = \frac{T_0}{3} + \frac{T_{\text{eff}}}{3}$$
$$\because T_s = T_0 + T_{\text{eff}}$$
$$T_{\text{offset}} = \frac{T_s}{3}$$

Similarly, the T_{offset} times can be calculated for the OFF sequence in the other sectors also and this works out to be equal to $T_s/3$ irrespective of the sector in which the tip of the reference vector is located. This means that a simple relocation of the effective time period within the sampling time period eliminates the zero-sequence voltage in the average sense. Thus, the degree of freedom in the placement of effective time period and the observation that certain space vector combinations have a zero value of zero-sequence voltages is exploited to the advantage in the proposed PWM strategy. However, such a non-centre-spaced PWM results in a higher current ripple and consequently a higher THD. The effects of such non-centre-spaced PWM techniques are discussed in detail in Holmes [18]. This PWM algorithm also offers a second degree of freedom in the choice of number of samples in the duration of 60°. If this number is even, all the even harmonics in the motor phase voltage are suppressed. On the other hand, if this number is odd, all the odd harmonics in the motor phase voltage are suppressed. This assertion is based on the spectra presented in Fig. 6. However, in motor drive applications it is not advisable to have even harmonics. Thus, in the present work, eight samples for 60° (i.e. 48 samples per cycle) are chosen for experimentation. The traces of triplen harmonics in the motor phase voltage, shown in Fig. 6, are because of the side-bands associated with the switching. Fig. 7*a* shows sector 8. From equation 2b, it may be noted that x can assume a maximum value of 1, which defines the limiting case for the applicability of the proposed PWM scheme. It may be noted in this limiting case ($x = 1$), $T_2 = T_0$. From Fig. 7*a*, it is evident that all the points situated on the straight line UH, such as 'Y', are equidistant to the vertices A and B. This means that if the sample is situated on this locus, appropriate vector combinations located at A and B are to be switched for equal time duration, thus making $T_2 = T_0$. It is therefore evident that all the samples situated within the shaded region of Fig. 7*a* are constructed by clamping one of the inverters with the state corresponding to those available at the location A. On the other hand, for all the other samples situated in the unshaded portion of Fig. 7*a*, B is the NSHC. Similar observations can be made for the other two sectors as well (Fig. 7*b* and *c*). Fig. 7*d* shows the jurisdiction of the SHC 'A'. From the above discussion it is clear that if the sample is situated in the triangle HSG, it cannot be realised with the proposed PWM algorithm. This means, to generate the rated motor voltage from the dual-inverter configuration, with a single power supply, the DC link voltage is to be slightly enhanced. Consequently, the hexagon, HJLNQS defines the boundary of operation with the proposed PWM scheme and the boundary of linear modulation corresponds to the biggest circle inscribed in the hexagon [8]. It is shown in Somasekhar *et al.* [8] and Baiju *et al.* [11] that the DC link voltage with and without electrical isolation are in the ratio of $1:(2/\sqrt{3})$, which is the ratio of the radii of the biggest circle in the hexagon GIKMPR and HJLNQS (Fig. 3). In other words, if it is intended to operate with electrical isolation, one needs two power supplies, each of $(V_{\text{dc}}/2)V$ while only one power supply

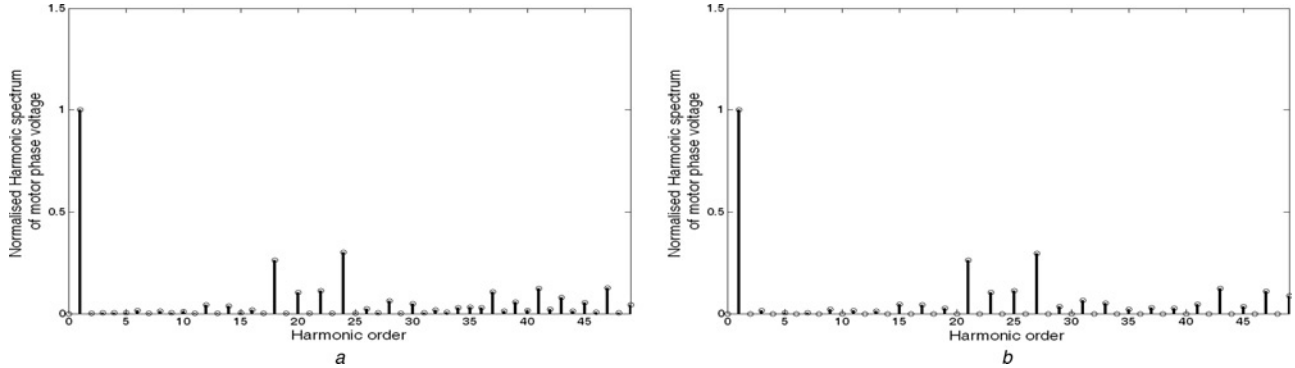

Fig. 6 *Normalised harmonic spectrum of motor phase voltage with the number of samples in 60° equal to 7 (left) and 8 (right)*

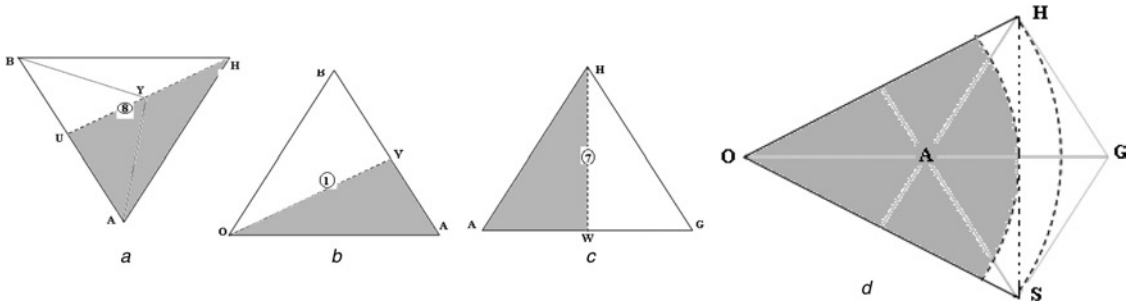

Fig. 7 *Boundaries showing the vicinity of the SHCs 'A' when the tip of the reference falls in (a) sector 8, (b) sector 1, (c) sector 7 and (d) vicinity under SHC 'A'*

of $(V_{dc}/\sqrt{3})V$ is needed with an enhancement of about 15% with the proposed PWM algorithm (where V_{dc} corresponds to OG, Fig. 3).

In any practical drive system, during the transient conditions, the controller could demand a higher voltage than what the inverter is capable of supplying. In such a situation, the tip of the reference vector would be situated outside the boundary of the hexagon HJLNQS. In such a situation, the instantaneous phase reference voltages v_a^*, v_b^* and v_c^* are emended so that the tip of the modified reference vector is situated on the hexagon HJLNQS. Fig. 8*a* depicts the original reference vector and its amended counterpart. Fig. 8*a* also shows the loci of the reference space vector corresponding to the modulation indices, corresponding to 0.4 and 0.7 (where the modulation index is represented as m_i is defined as the ratio of $|V_{sr}|/V_{dc}$), wherein the dual-inverter system operates in the range of linear modulation. When $m_i = 0.4$ and 0.7, the instantaneous phase reference voltages do not need to be amended as they would be sinusoidal and the dual-inverter system operates in the linear modulation. Fig. 8*b* shows the instantaneous phase reference voltages corresponding to over-modulation, wherein the tip of the reference vector traverses the outer hexagon GIKMPR rather than the desired hexagon HJLNQS. The over-modulation described in Chung *et al.* [17] would force the tip of the reference vector to trace the hexagon GIKMPR and is not described here in the interest of brevity. From Fig. 8a, it may be noted that the instantaneous *a*-phase reference voltage corresponding to the straight line SH is given by

$$v_a^* = \tfrac{2}{3} \times \tfrac{3}{4} \times V_{dc} = \frac{V_{dc}}{2} \text{ or } \frac{v_a^*}{V_{dc}} = 0.5$$

In other words, v_a^* is to be clamped to $0.5V_{dc}$, to trace the straight line SH. The excess voltage $(v_{a,\text{original}}^* - v_{a,\text{amended}}^*)$ is redistributed to the other two phase reference voltages (v_a^* and v_b^*) to satisfy the three-phase constraint $v_{a,\text{amended}}^* + v_{b,\text{amended}}^* + v_{c,\text{amended}}^* = 0$. It should be noted that to trace the upper half of the straight line segment SH, all the space vector locations situated in the nearest proximity (A, G and H in this case) are switched. However, it is possible and is a better proposition to switch the locations S and H only to trace this line segment, as the space vector combinations at S and H have a zero sequence voltage of zero [10].

4 Results and discussion

The proposed PWM scheme is first simulated using MATLAB and the results are verified by implementing the scheme on a 5-HP, three-phase induction motor with V/f control for different reference voltages over the entire speed range. The gating pulses to the dual-inverter are

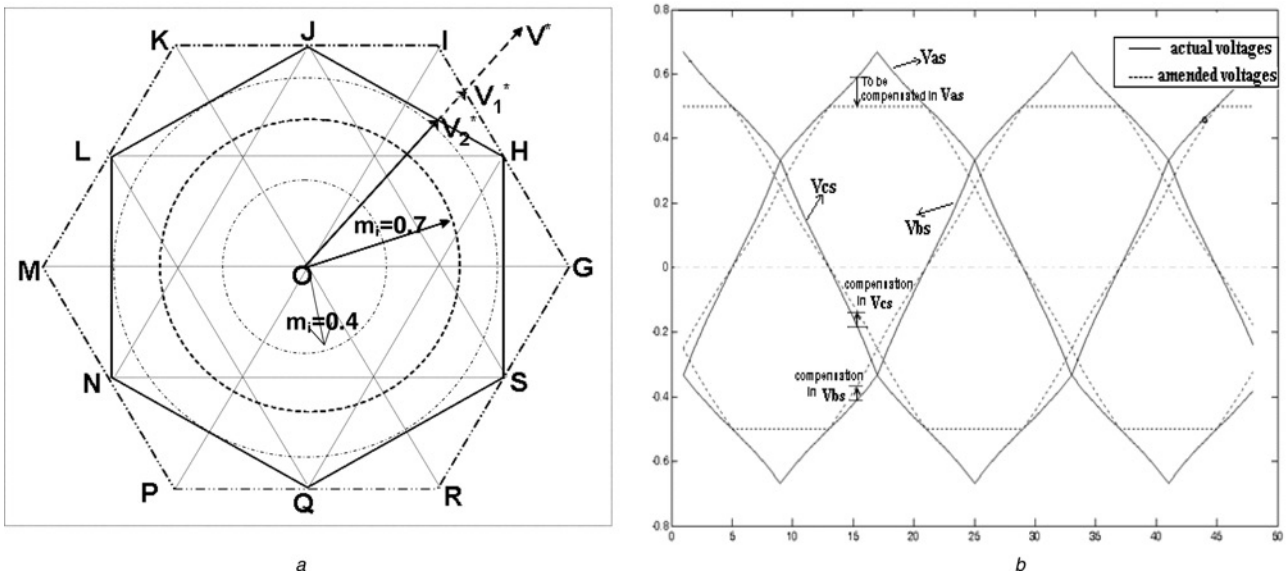

Fig. 8 *Reference vectors and voltages*

a The locus of tips of the reference vectors in different regions (left)
b Actual and adjusted three-phase reference voltages (right)

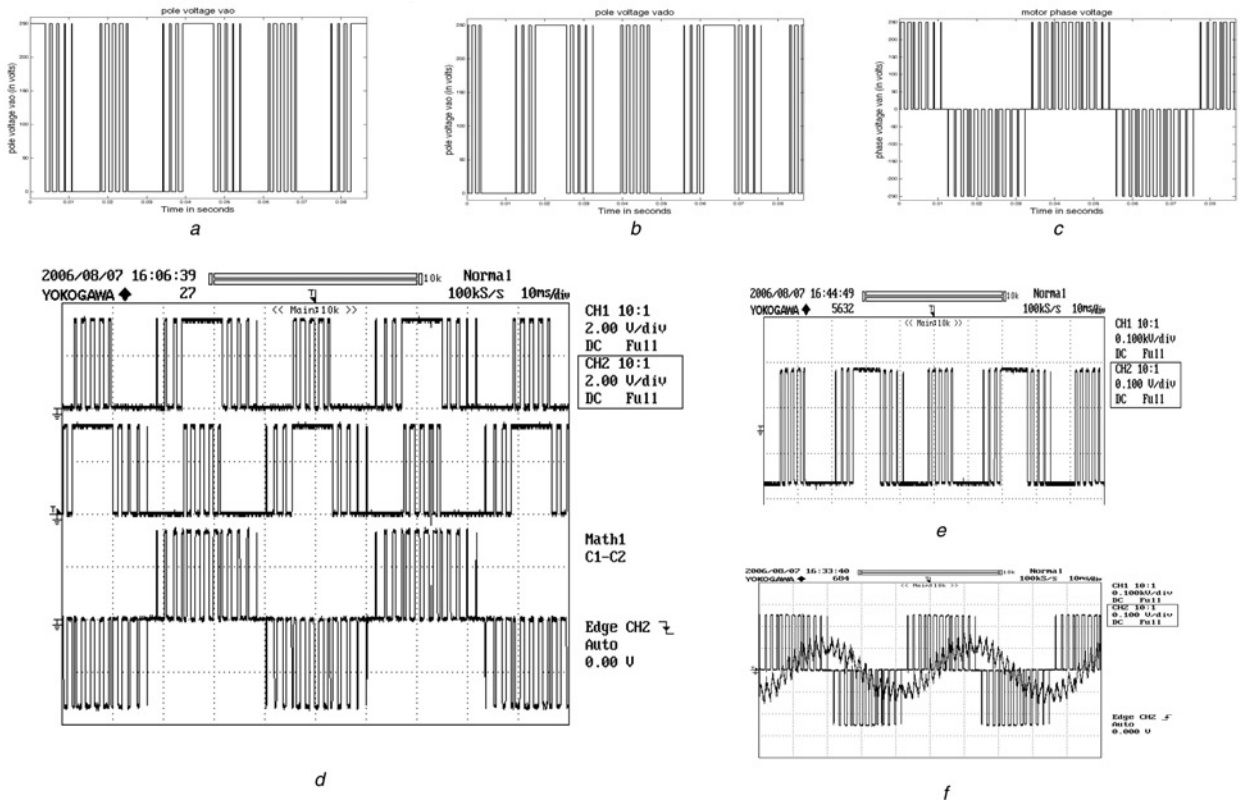

Fig. 9 *Simulated and experimentally obtained waveforms for* $m_i = 0.4$

a Simulated waveform of a-phase pole voltage of inverter-1, v_{ao}
b Simulated waveform of *a*-phase pole voltage of inverter-2, $v_{a'o}$
c Simulated waveform of phase voltage, v_{an}
d Gate pulses generated by the DSP
e Experimentally obtained waveform of *a*-phase pole voltage of inverter-1, v_{ao}
f Experimentally obtained *a*-phase phase voltage, v_{an} and no-load motor phase current

generated using the TMS320LF2407A Digital Signal Processor. A fixed number of 48 samples per cycle are employed for the implementation of proposed scheme in the entire operating range. A DC link voltage of 250 V is used for experimentation.

The simulated waveforms of the *a*-phase pole voltages of the two inverters (v_{ao} and $v_{a'o}$) and the *a*-phase motor phase voltage for an m_i of 0.4 are shown in Fig. 9*a–c*, respectively. The gating signals generated by the DSP, depicting the *a*-phase pole voltages of the two inverters along with the motor phase voltage that is the difference of the two pole voltages (bottom trace) is shown in Fig. 9*d*. It may be noted from Fig. 9*d* that, when one inverter is switched the other is clamped. The experimentally obtained *a*-phase pole voltage of inverter-1 and the motor phase voltage for the same m_i of 0.4 are shown in Fig. 9*e* and *f*. The no-load motor phase current is also shown in Fig. 9*f*. Similarly, the simulated and experimental results for $m_i = 0.7$ and over-modulation are shown in Figs. 10 and 11, respectively.

With the alternate-SHC PWM switching scheme for the dual-inverter fed from isolated DC power supplies (placing the effective-time in the centre within the sampling interval) as reported in Somasekhar *et al*. [14], the experimentally obtained results of the motor-phase voltage (top-trace) and the no-load motor-phase current (bottom-trace) for $m_i = 0.4$, 0.7 and over-modulation are shown in Fig. 12*a–c*, respectively. Fig. 12*d–f* show the experimentally obtained, motor phase voltage (top trace) and the motor phase current (bottom trace) for the modulation indices of 0.4, 0.7 and over-modulation when the same PWM scheme is applied to the dual-inverter fed open-end winding induction motor drive with a single DC power supply (Fig. 1). The waveforms shown in Fig. 12*d–f* are taken at a reduced DC link voltage of 150 V. It may also be noted that at such a reduced voltage itself the triplen content in the motor phase current is strong.

The waveform shown in Fig 12*g–i* are the ones shown here for quick reference (also shown in Figs. 9*f*, 10*f* and 11*f*) for $m_i = 0.4$, 0.7 and over-modulation, respectively, with the PWM scheme proposed in this paper. It may be noted that the voltage waveforms in Fig. 12*f* and *i* are different as two different hexagons are traced, the hexagon GIKMPR in with electrical isolation and HJLNQS without the same (Fig. 8*a*). It is evident from the current waveforms that the triplen harmonic content is reduced. This demonstrates the effectiveness of the proposed effective-time relocation algorithm within the sampling time interval. From Fig. 12, it is evident that the application of the PWM scheme suggested in Somasekhar *et al*. [14] to the power circuit topology shown in Fig. 1 results in a phase current that is rich in zero-sequence content (Fig. 12*d–f*). When two isolated power supplies are employed to power individual inverters, the zero-sequence contents are suppressed altogether and results in the best waveforms for the phase current (Fig. 12*a–c*). Thus, the PWM scheme suggested in this paper, although results in a slight compromise when compared with centre-spaced space vector modulation strategy [14], offers the advantage of operating with only one DC power supply. Also, this PWM strategy enables the realisation of true three-level operation for an open-end winding scheme, using all the space vector locations with a single DC power supply, unlike the PWM scheme proposed in Somasekhar *et al*. [10] and Baiju *et al*. [11].

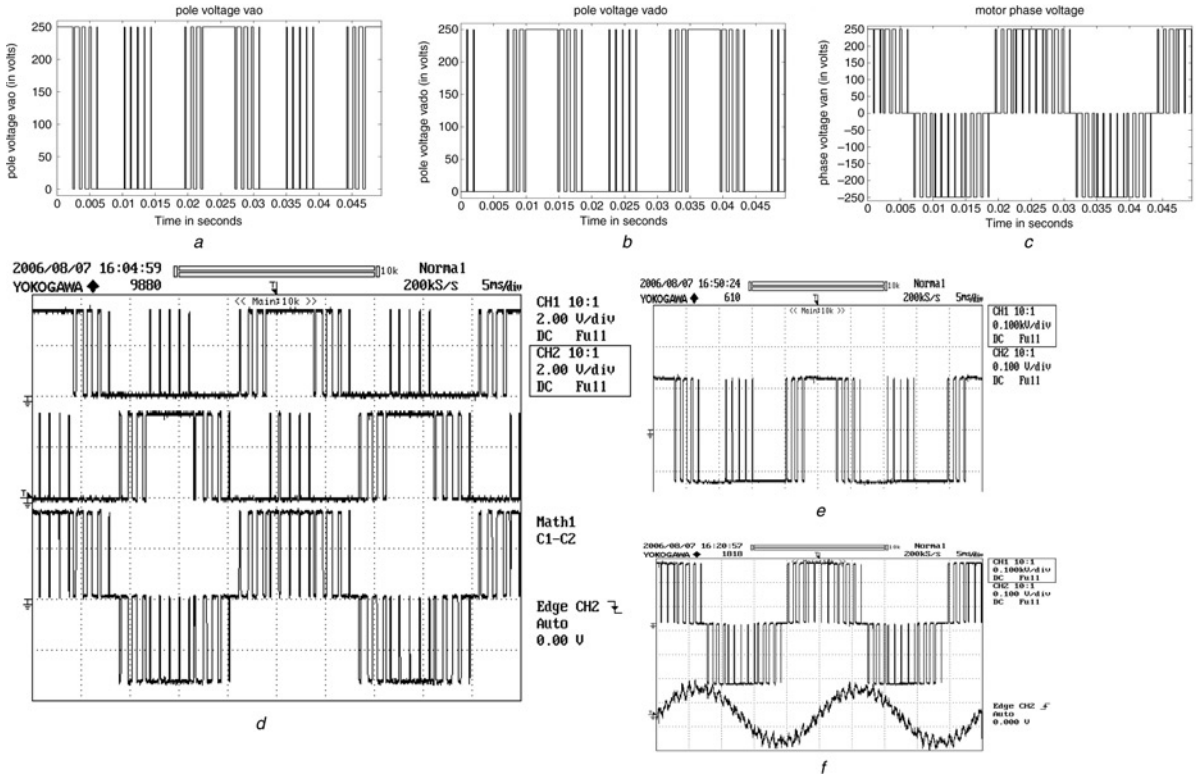

Fig. 10 *Simulated and experimentally obtained waveforms for* $m_i = 0.7$

a Simulated waveform of *a*-phase pole voltage of inverter-1, v_{ao}
b Simulated waveform of *a*-phase pole voltage of inverter-2, $v_{a'o}$
c Simulated waveform of phase voltage, v_{an}
d Gate pulses generated by the DSP
e Experimentally obtained waveform of *a*-phase pole voltage of inverter-1, v_{ao}
f Experimentally obtained *a*-phase phase voltage, v_{an} and no-load motor phase current

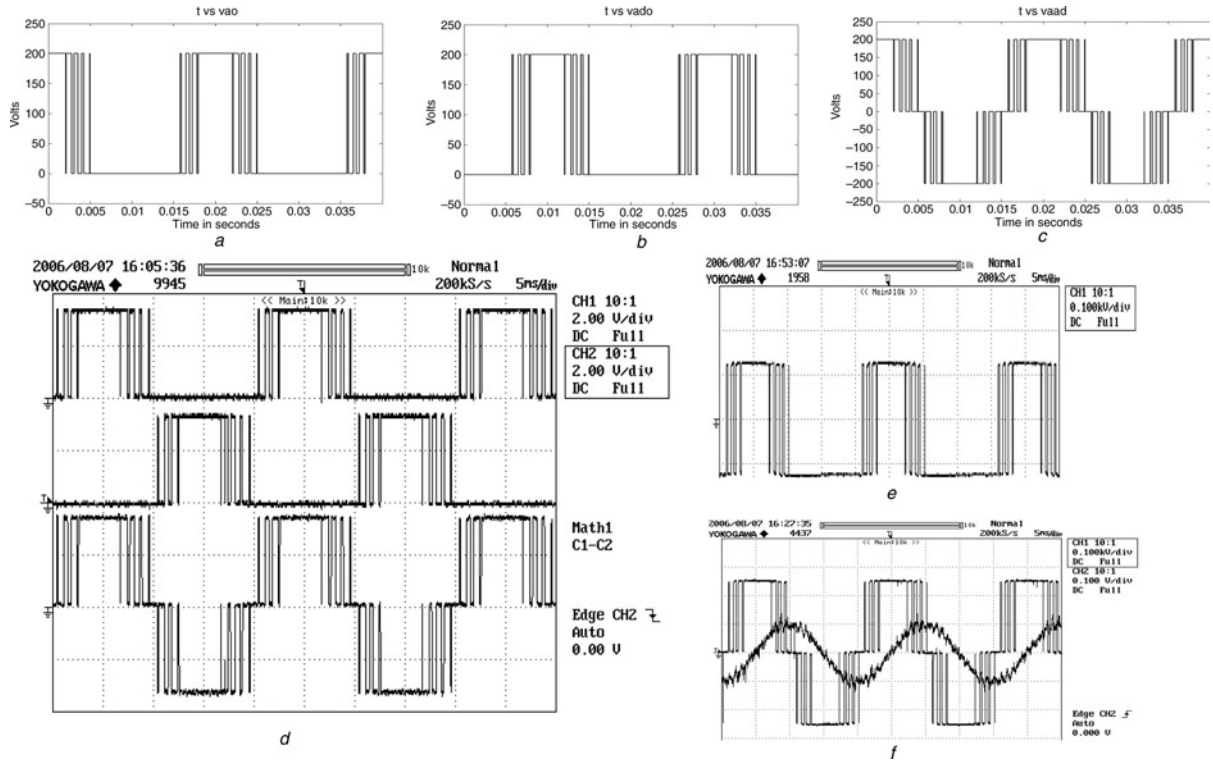

Fig. 11 *Simulated and experimentally obtained waveforms for over-modulation*

a Simulated waveform of *a*-phase pole voltage of inverter-1, v_{ao}
b Simulated waveform of *a*-phase pole voltage of inverter-2, $v_{a'o}$
c Simulated waveform of phase voltage, v_{an}
d Gate pulses generated by the DSP
e Experimentally obtained waveform of *a*-phase pole voltage of inverter-1, v_{ao}
f Experimentally obtained *a*-phase phase voltage, v_{an} and no-load motor phase current

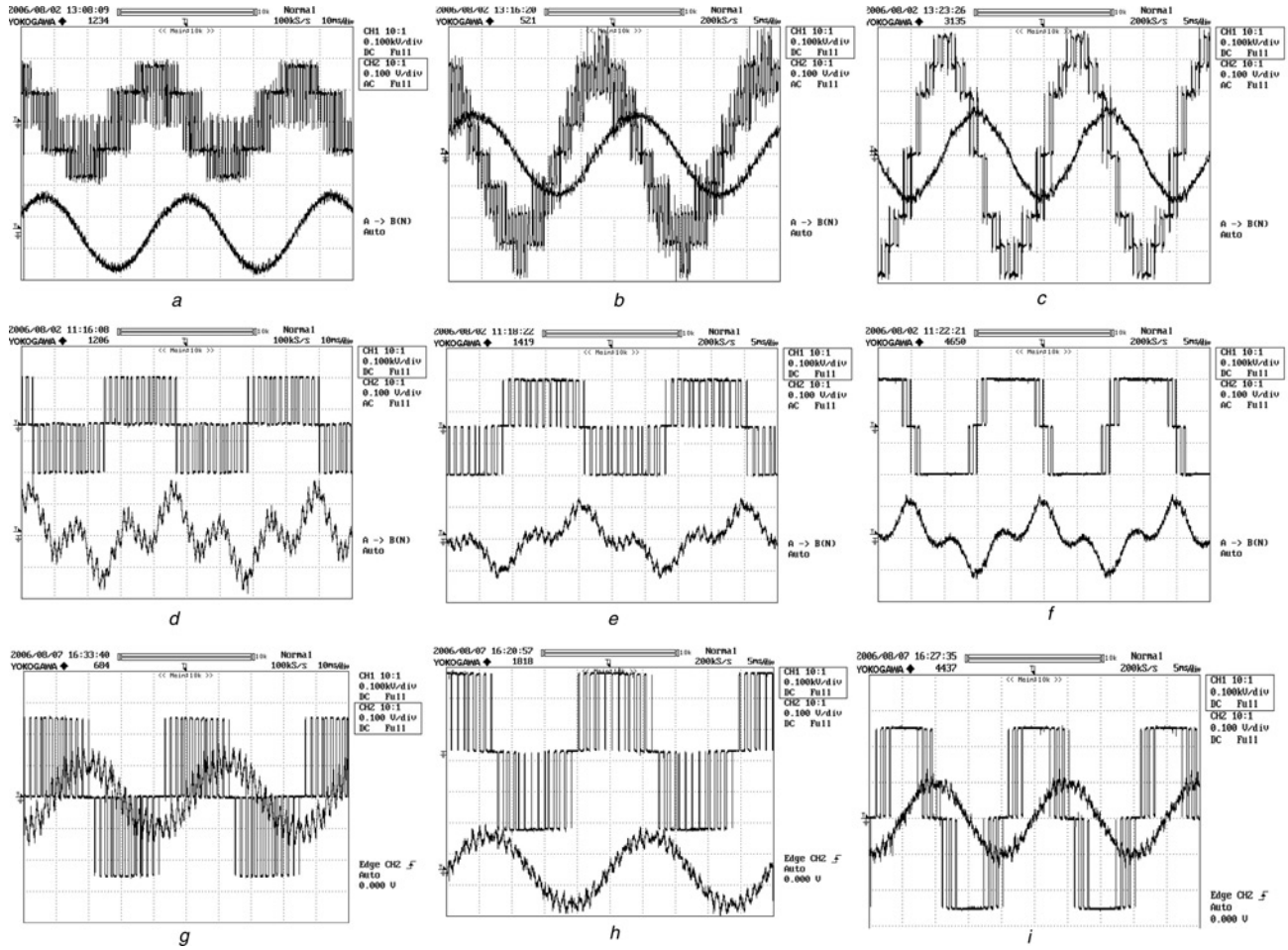

Fig. 12 *Experimentally obtained motor phase voltage v_{an} (top-trace) and the motor phase current (bottom-trace)*

a for $m_i = 0.4$ with isolated DC power supplies
b for $m_i = 0.7$ with isolated DC power supplies
c for over-modulation with isolated DC power supplies
d for $m_i = 0.4$ with a single DC power supply
e for $m_i = 0.7$ with a single DC power supply
f for over-modulation with a single DC power supply
g for $m_i = 0.4$ with the PWM scheme proposed in this paper and the power circuit in Fig. 1
h for $m_i = 0.7$ with the PWM scheme proposed in this paper and the power circuit in Fig. 1
i for over-modulation with the PWM scheme proposed in this paper and the power circuit in Fig. 1

In this PWM scheme, one inverter is clamped while the other is switched. This results in half the switching frequency compared with the one proposed in Somasekhar *et al*. [10] and Baiju *et al*. [11].

5 Conclusion

In this paper, a space vector-based PWM scheme is proposed. This scheme facilitates the operation of a dual-inverter fed open-end winding induction motor with a single power supply. This scheme eliminates the necessity for the transformer isolation as in Shivakumar *et al*. [7] and the auxiliary switches as in Somasekhar *et al*. [8, 9]. It is shown that it is feasible, in principle, to employ all the space vector locations (19 in numbers) for three-level inversion. This is achieved with a simple relocation of the effective time within a sampling time period. With the proposed PWM scheme, only one inverter is switched in a sampling time interval unlike the schemes proposed in Somasekhar *et al*. [10] and Oleschuk *et al*. [12]. These advantages could outweigh the increase of the DC link voltage and the current ripple in the motor phases.

6 References

1 Nabae, A., Takahashi, I., and Akagi, H.: 'A neutral-point clamped PWM inverter', *IEEE-Trans. Ind. Appl.*, 1981, **17**, (5), pp. 518–523
2 Maynard, T.A., and Foch,: 'Multi-level conversion: high voltage choppers and voltage source inverters'. Conf. Proc. IEEE PESC, 1992, pp. 397–403
3 Tolbert, L.M., Peng, F.Z., and Habetler, T.G.: 'Multilevel converters for large electric drives', *IEEE Trans. Ind. Appl.*, 1999, **35**, (1), pp. 36–44
4 Manjrakar, M.D., and Lipo, T.A.: 'A hybrid multilevel inverter topology for drive applications'. Conf. Proc. IEEE-APEC, 1998, pp. 523–529
5 Manjrekar, M.D., Steimer, P.K., and Lipo, T.A.: 'Hybrid multilevel power conversion system: a competitive solution for high-power applications', *IEEE Trans. Ind. Appl.*, 2000, **36**, (3), pp. 834–841
6 Stemmler, H., and Guggenbach, P.: 'Configurations of high-power voltage source inverter drives'. Proc. EPE Conf., 1993, pp. 7–14
7 Shivakumar, E.G., Gopakumar, K., Sinha, S.K., Pittet, A., and Ranganathan, V.T.: 'Space vector control of dual inverter fed open-end winding induction motor drive', *EPE J.*, 2002, **12**, (1), pp. 9–18
8 Somasekhar, V.T., Gopakumar, K., Pittet, A., and Ranganathan, V.T.: 'PWM inverter switching strategy for a dual two-level inverter fed open-end winding induction motor drive with a switched neutral', *IEE Proc., Electr. Power Appl.*, 2002, **149**, (2), pp. 152–160
9 Somasekhar, V.T., Baiju, M.R., and Gopakumar, K.: 'Dual two level inverter scheme for an open-end winding induction motor drive with a

single DC power supply and improved DC bus utilization', *IEE Proc., Electr. Power Appl.*, 2004, **151**, (2), pp. 230–238
10 Somasekhar, V.T., Gopakumar, K., Shivakumar, E.G., and Sinha, S.K.: 'A space vector modulation scheme for a dual two level inverter fed an open-end winding induction motor drive for the elimination of zero sequence currents', *EPE J.*, 2002, **12**, (2), pp. 26–36
11 Baiju, M.R., Mohapatra, K.K., Kanchan, R.S., and Gopakumar, K.: 'A dual two-level inverter scheme with common mode voltage elimination for an induction motor drive', *IEEE Trans. Power Electron.*, 2004, **19**, (3), pp. 794–805
12 Oleschuk, V., Bose, B.K., and Stankovic, A.M.: 'Phase-shift-based synchronous modulation of dual-inverters for an open-end winding induction motor drive with elimination of zero sequence currents'. Conf. Proc. IEEE-PEDS, 2005, pp. 325–330
13 Somasekhar, V.T., and Srinivas, S.: 'Switching algorithms for a dual inverter fed open-end winding induction motor drive'. Conf. Proc. IEEE-IICPE, Mumbai, India, 2004
14 Somasekhar, V.T., Srinivas, S., and Gopakumar, K.: 'A space vector based PWM switching scheme for the reduction of common-mode voltages for a dual inverter fed open-end winding induction motor drive'. Conf. Proc. IEEE-PESC, Recife, Brazil, 2005, pp. 816–821
15 Srinivas, S., and Somasekhar, V.T.: 'A new alternate-inverter PWM switching strategy for reducing the common-mode voltages for a dual-inverter fed open-end winding induction motor drive'. Conf. Proc. IPEC, Niigata, Japan, 2005, pp. 1460–1465
16 Kim, J.-S., and Sul, S.-K.: 'A novel voltage modulation technique of the space vector PWM'. Conf. Proc. IPEC, 1995, pp. 742–747
17 Chung, D.-W., Kim, J.-S., and Sul, S.-K.: 'Unified voltage modulation technique for real-time three-phase power conversion', *IEEE Trans. Ind. Appl.*, 1998, **34**, (2), pp. 374–380
18 Holmes, D.G.: 'The significance of zero-space vector placement for carrier-based PWM schemes', *IEEE Trans. Ind. Appl.*, 1996, **32**, (5), pp. 1122–1129